On-chip micro-supercapacitors for operation in a wide temperature range

Peihua Huang [a,b,c], David Pech [a,b], Rongying Lin [c,d], John K. McDonough [e,f], Magali Brunet [a,b], Pierre-Louis Taberna [c,d], Yury Gogotsi [e,f], Patrice Simon [c,d,*]

[a] CNRS, LAAS, 7 avenue du colonel Roche, F-31400 Toulouse, France
[b] Univ de Toulouse, LAAS, F-31400 Toulouse, France
[c] Univ Paul Sabatier, CIRIMAT UMR-CNRS 5085, F-31062 Toulouse Cedex 4, France
[d] Réseau sur le Stockage Electrochimique de l'Energie (RS2E), FR CNRS n°3459, France
[e] Department of Materials Science Engineering, Drexel University, Philadelphia, PA 19104, USA
[f] A.J. Drexel Nanotechnology Institute, Drexel University, Philadelphia, PA 19104, USA

A B S T R A C T

Onion-like carbon (OLC) based micro-supercapacitor electrodes prepared by electrophoretic deposition (EPD) were combined with a eutectic mixture of ionic liquids (IL), producing a micro-supercapacitor which is able to function from −50 °C to 80 °C. This device was electrochemically characterized by cyclic voltammetry and electrochemical impedance spectroscopy at different scan rates and different temperatures. At 20 °C, a capacitance of 1.1 mF.cm^{-2} per footprint area of device at 200 mV.s^{-1} within 3.7 V was measured, hence a specific energy of 15 mJ.cm^{-2} and a specific power of 240 mW.cm^{-2}. At −50 °C, 76% of the capacitance was maintained at 10 mV.s^{-1} within 3.7 V. By integrating with IL, this micro-supercapacitor can be potentially used in portable electronic devices that are required to work under temperature extremes.

Keywords:
Micro-supercapacitors
Ionic liquid electrolyte
Large voltage window
Large operation temperature

1. Introduction

The increasing popularity of portable electronic devices demands development of micro-size power sources which could save space for other electronic components and further decrease the device size. Micro-batteries have been developed for this purpose since the early 1990s [1,2]. Although the use of nanomaterials [3], thin-films [4] or 3D structures [5] allows substantial improvement in the diffusion limitations of these redox-based systems, the power limitation is still a concern for Li-ion batteries. Electrochemical capacitors (supercapacitors) that store energy by adsorption of ions from an electrolyte are good alternative or supplement to batteries in high-power applications. The integration of micro-supercapacitors on a chip is thus an increasing field of research supported by the increasing development of embedded micro-systems.

Portable electronic devices are expected to work at different locations and thus at different temperatures. Additionally, in some applications (aeronautic and aerospace) the electronic systems have to experience fast change in temperature from the ambient on the earth surface (20–40 °C) to very low temperatures (down to −50 °C) at high altitude requiring the micro-power source to be tolerant to large temperature fluctuations. The temperature tolerance of carbon-based micro-supercapacitors mostly depends on the choice of the electrolyte, there is thus a key need for designing micro-supercapacitors with a wide temperature range tolerant electrolyte.

Aqueous electrolytes with voltage window less than 1 V have low viscosity thus high power, but the small voltage window limits the energy density (E) by $E = \frac{1}{2} CV^2$ where C is the cell capacitance and V the cell potential. Additionally, low temperature operation is generally limited to about 0 °C. Acetonitrile (AN) or propylene carbonate (PC) based organic electrolytes exhibit a voltage window of 2.5–3 V. Despite lower ionic conductivity, the high voltage window of non-aqueous electrolytes increases their power and energy performance. However, the operation temperature is limited to −20 to 70 °C for PC or to −40 to 65 °C range for AN based electrolytes.

Room temperature ionic liquids (RTILs), are salts with a melting point below room temperature. Because of the absence of solvent, they are stable over a large range of temperatures (up to more than 300 °C) and such electrolytes show a wide electrochemical voltage window (beyond 4 V) [6]. The main drawbacks of RTILs are i) the melting point which is close to 0 °C in most of the cases, ii) high viscosity, and iii) low ionic conductivity (few mS/cm at room temperature). These features have restricted the use of RTILs in supercapacitors to high temperature applications, typically above 50 °C [6–8].

Recently, a eutectic mixture of ionic liquids (ILM) N-methyl-N-propylpiperidiniumbis[fluorosulfonyl]imide ($PIP_{13}FSI$) and N-butyl-N-methylpyrrolidiniumbis[fluorosulfonyl]imide ($PYR_{14}FSI$) in the 1:1 ratio was reported to show no freezing down to −80 °C. Using exohedral carbons with fully accessible surface area like carbon nanotubes (CNTs), onion like carbon (OLC) or activated graphene, supercapacitors

* Corresponding author at: Univ Paul Sabatier, CIRIMAT UMR-CNRS 5085, F-31062 Toulouse Cedex 4, France.
E-mail address: simon@chimie.ups-tlse.fr (P. Simon).

http://dx.doi.org/10.1016/j.elecom.2013.09.003

assembled with this $PIP_{13}FSI$:$PYR_{14}FSI$ electrolyte mixture were able for the first time to operate within the temperature range, from −50 up to 100 °C [9,10].

On the other hand, an OLC-based on-chip micro-supercapacitor prepared by EPD has shown ultrahigh power delivery in 1 M NEt_4BF_4/PC electrolyte [11].

In this paper we report for the first time the use of an IL eutectic mixture combined with OLC for assembling a microsupercapacitor that can work from −50 to 80 °C within a large voltage window (3.7 V at room temperature). Beyond the improved performance, the combination of neat IL mixture and OLC carbons offers important key features such as enhanced flexibility for packaging because of the absence of any solvent (neat ionic liquids), or the possibility of using temperatures as high as 250 °C for micro-supercapacitor processing (like encountered with the flow or reverse flow soldering processes).

2. Materials and experimental

2.1. Electrophoretic deposition

Micro-supercapacitors were prepared using the EPD technique, from a suspension of OLC particles which were produced by annealing detonation nanodiamond powder at 1800 °C. The suspension contained 0.3 wt% of OLC (electrode material), 0.03 wt% of $MgCl_2$ in a mixture of 95% of ethanol and 5% of water [11]. $MgCl_2$ in water produces $Mg(OH)^+$ cations to charge OLC particles and form a stable suspension.

A well-defined interdigitated pattern of gold current collectors with a footprint area of 0.25 cm^2 and interspace of 150 μm deposited on a Si wafer was used as the electrode for EPD as shown in Fig. 1.a. The pattern size and design were defined according to a previous work from Pech et al. [12].

A layer of OLC of 7 μm in thickness was then deposited between two electrodes with a design of four fingers (two fingers per electrode) as shown in Fig. 1b. The sample was then outgassed under 250 °C overnight to remove the gas trapped in the deposited layer, resulting in a smooth and continuous film. The micro-supercapacitor was then assembled onto a support with wire bonding to facilitate electrochemical characterization.

2.2. Electrochemical characterization

Before electrochemical characterization, the sample was kept in vacuum oven at 130 °C overnight to remove water. Electrochemical characterization was carried out under Ar atmosphere (H_2O and O_2 level lower than 0.1 ppm) with a Biologic VMP2 potentiostat. Electrochemical impedance spectroscopy (EIS) measurements were performed at the rest potential (0 V) from 500 kHz down to 10 mHz with a sinusoidal perturbation potential signal of −/+300 mV. Cyclic voltammograms (CVs) were recorded at −50 °C, −40 °C, 20 °C and 80 °C, at different scan rates within a voltage window of 3.7 V, except at 80 °C (2.8 V).

3. Results and discussion

Fig. 2 shows the Nyquist plots of the micro-supercapacitor in the $PIP_{13}FSI$:$PYR_{14}FSI$ 1:1 IL electrolyte mixture at −50 °C and 20 °C. The Nyquist plot at 20 °C is consistent with a capacitive behavior, with a sharp increase of the imaginary part of the impedance at low frequency. However, a slight deviation from the theoretical 90° vertical line is observed, indicating the presence of a small leakage current, possibly linked with a few micro-short circuits between the electrodes resulting from the deposit of carbon particles in the current collector interspace region. The Nyquist plot at −50 °C shows the presence of a high frequency loop, shifting the capacitive behavior to larger series resistance value. This loop originated from the IL electrolyte mixture decrease in conductivity, linked with the increase of the viscosity [13], thus limiting the ion transfer and mobility.

The inset shows the change of the capacitance calculated from EIS data [14] with the frequency indicating that the capacitance of the micro-supercapacitor in ILM at 20 °C (0.15 mF) is much higher than the one at −50 °C (0.10 mF). At this temperature, the ILM electrolyte turns into a gel with limited ion mobility, thus the maximum capacitance could not be achieved. This absence of saturation of the capacitance at low frequency is assumed to originate from the OLC electrode, where a charge distribution in the inter-particle porosity effect can be observed because of the low conductivity of the electrolyte at −40 and −50 °C. In contrast, at 20 °C, there is a quasi-plateau at low frequency end. The plateau is sloping, showing the presence of a small leakage current as already mentioned; this leakage current prevents from reaching the saturation (full capacitance) of the capacitance at low frequency. The presence of leakage current was identified by cyclic voltammetry at low scan rate (1 mV/s), that shows a sloping behavior (not shown).

These observations support the need for an optimization of the test vehicle (cell geometry) for improving the leakage current by playing with the inter-space distance, electrode thickness and current collector lengths and widths. Such optimization in the cell geometry would also allow decreasing the 300-mV amplitude waveform used for the EIS measurements at the OCV to a more conventional value of 10–20 mV, thus being closer to the equilibrium of the system during the measurements.

CVs were recorded at all temperatures (Fig. 3). At 20 °C, the CV plot shown in Fig. 3a indicates a typical capacitive behavior with a rectangular shape at 200 $mV.s^{-1}$ within a large voltage window of 3.7 V; this voltage window increase is an important improvement when compared with the literature [11,15,16]. Beyond 3.5 V, the electrolyte oxidation starts to occur as can be seen from increase of the

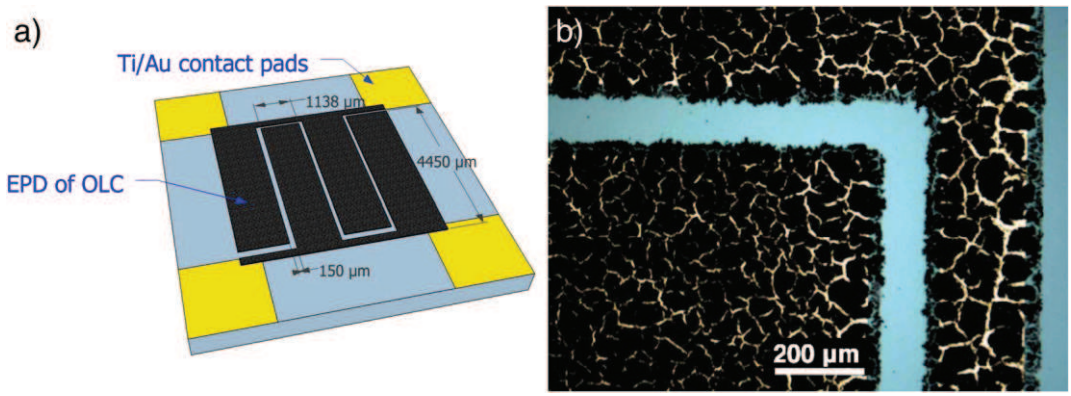

Fig. 1. a) Schematic picture of on-chip micro-supercapacitor with OLC as electrode material prepared by EPD and b) microscopic picture.

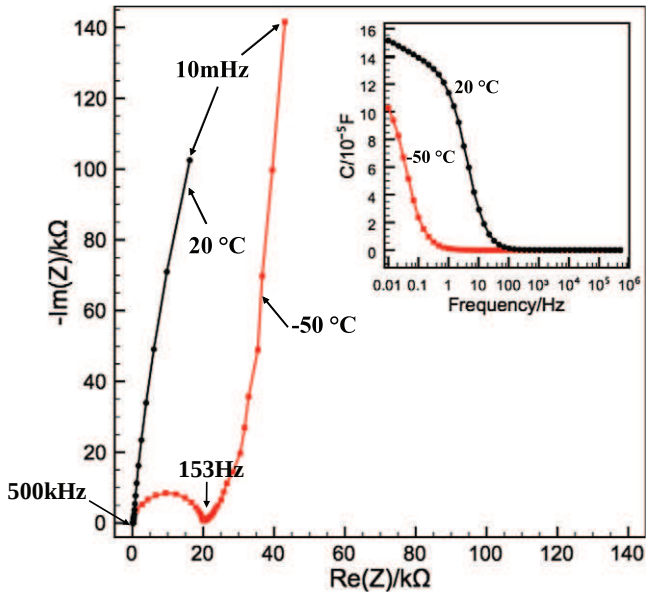

Fig. 2. Nyquist plot of OLC based micro-supercapacitor in ILM at −50 °C and 20 °C and the change of capacitance calculated from EIS data [14] (inset).

current. Fig. 3b shows the CV plots of the OLC based micro-supercapacitor in ILM at 1 V.s^{-1} at 20 °C and 80 °C, up to 2.8 V. Ideal capacitive behaviors are presented with a rectangular CV shape at both temperatures. The cell voltage was limited to 2.8 V because of the enhanced electrolyte oxidation on gold current collectors at the elevated temperature.

At low temperatures, −50 °C and −40 °C, the CV plots at 10 mV.s^{-1} (Fig. 3c) show a rectangular shape up to 3.7 V, thus in line with the decreased oxidation rate of the electrolyte at low temperatures. In previously reported data of a 4 cm^2 cell, the CV was much distorted at −50 °C within the same voltage window even at 1 mV.s^{-1} with the same electrode material and electrolyte [9]. Still, the combination of a micro-supercapacitors device and IL electrolyte mixture led to an extended operation temperature range of the micro-device.

At 20 °C, a capacitance of 1.1 mF.cm^{-2} per footprint area of device in ILM at 200 mV.s^{-1} within 3.7 V was measured, leading to a specific energy of 7.5 mJ.cm^{-2} and a power density of 240 mW.cm^{-2}. Both the capacitance and energy density are higher than that in PC-based electrolyte, the latter mainly due to the extended voltage window. The power delivery was not as high as that when using PC-based electrolyte [11] because of the higher ionic resistance of ILM [9]. The footprint area capacitance is in the range of most reported carbon based micro-supercapacitors with thickness not exceeding few microns [17–19]. At −50 °C, a capacitance of 0.84 mF.cm^{-2} at 10 mV.s^{-1} was calculated, i.e. 76 % of the 20 °C value.

Volumetric capacitances of the micro-supercapacitor at different scan rates and different temperatures over 2.8 V are compared in Fig. 4. The volumetric capacitance of the micro-supercapacitor decreases with increasing scan rate, since the ohmic drop increases with the scan rate. Temperature plays an important role. The lower the temperature, the faster the capacitance decrease since at low temperature the ionic conductivity of the electrolyte decreases, thus the series resistance of the cell increases. At the same scan rate, the higher the temperature, the higher the capacitance. This is also linked with the increase of the ionic conductivity at high temperature, thus decreasing the cell ESR.

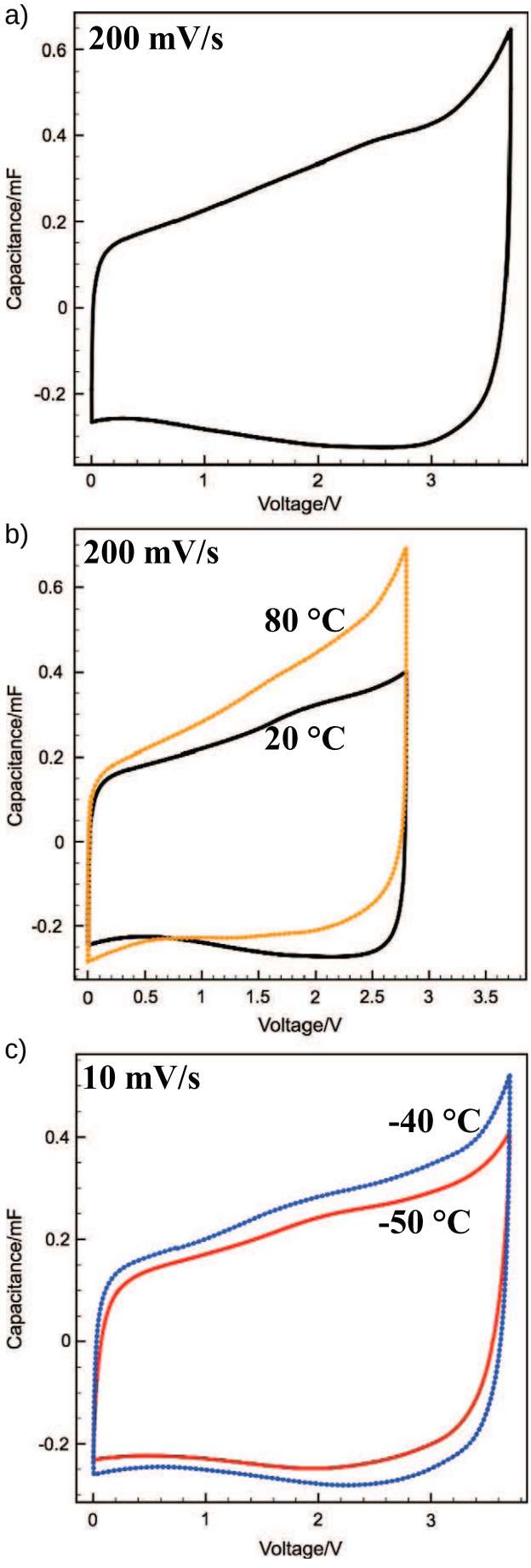

Fig. 3. CV plots of OLC based micro-supercapacitor in ILM a) at 20 °C within 3.7 V at 200 mV/s; b) at 20 °C and 80 °C within 2.8 V at 200 mV/s; c) at −50 °C and −40 °C within 3.7 V at 10 mV/s.

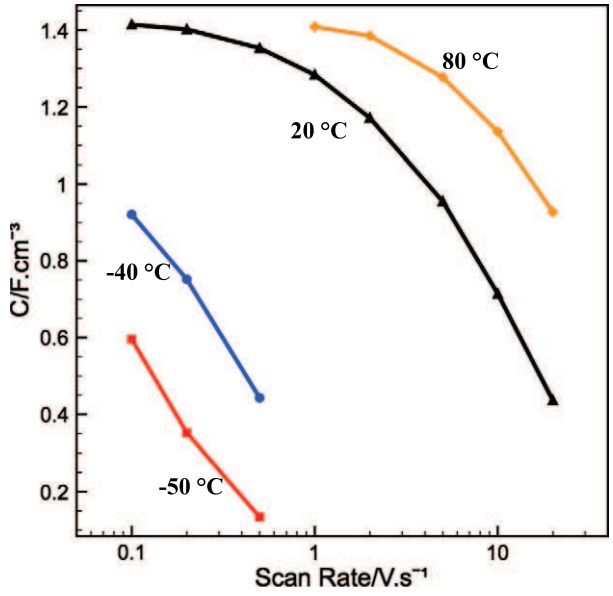

Fig. 4. Evolution of capacitance versus scan rate of OLC based micro-supercapacitor in ILM within 2.8 V at different temperatures.

4. Conclusions

A micro-supercapacitor working in a wide range of temperatures (from −50 up to 80 °C) has been fabricated *via* electrophoretic deposition of onion-like-carbon as electrode material combined with a eutectic mixture of ionic liquids as the electrolyte. The prepared micro-devices showed good performance at room temperature with a 1.1 $mF.cm^{-2}$ capacitance per footprint area of device at 200 $mV.s^{-1}$ within 3.7 V, hence a specific energy of 15 $mJ.cm^{-2}$ and a power density of 99 $mW.cm^{-2}$. Despite the presence of leakage current, the assembled devices were functional at low (−50 °C) and high (80 °C) temperatures with a moderate decrease in performance. The use of an optimized cell design, by playing with the inter-space distance, electrode thickness and current collector lengths and widths, would be needed for improving the leakage current. Low-temperature performance is better in micro-supercapacitors than its corresponding macroscopic devices using the same electrode material and the same electrolyte. This combination of the OLC based micro-supercapacitor design with the eutectic IL mixture electrolyte can address the micro-scale energy storage for portable devices for safe operation under temperature extremes.

Acknowledgment

We would like to thank the Partnership Universities Fund (PUF) for funding the US–French collaboration. Microfabrication was conducted in the Micro and nano technologies platform of LAAS-CNRS. P.H. was supported by a PhD grant from the PRES of the Université de Toulouse. PS acknowledges funding from the European Research Council (ERC-Advanced Grant 2011, Project 291543 — IONACES) and the Chair of Excellence 'Embedded multi-functional nanomaterials' from the EADS Foundation. Synthesis of carbon onions was done at Drexel University with support from the Fluid Interface Reactions, Structures and Transport (FIRST) Center, an Energy Frontier Research Center funded by the U.S. Department of Energy.

References

[1] W. Wang, M. Tian, A. Abdulagatov, S.M. George, Y.-C. Lee, R. Yang, Nano Lett. 12 (2011) 655–660.
[2] P. Simon, Y. Gogotsi, Nat. Mater. 7 (2008) 845–851.
[3] A.S. Arico, P. Bruce, B. Scrosati, J.M. Tarascon, W. Van Schalkwijk, Nat. Mater. 4 (2005) 366–377.
[4] J.W. Long, B. Dunn, D.R. Rolison, H.S. White, Chem. Rev. 104 (2004) 4463–4492.
[5] M. Roberts, P. Johns, J. Owen, D. Brandell, K. Edstrom, G. El Enany, C. Guery, D. Golodnitsky, M. Lacey, C. Lecoeur, H. Mazor, E. Peled, E. Perre, M.M. Shaijumon, P. Simon, P.-L. Taberna, J. Mater. Chem. 21 (2011) 9876–9890.
[6] M. Armand, F. Endres, D.R. MacFarlane, H. Ohno, B. Scrosati, Nat. Mater. 8 (2009) 621–629.
[7] C. Arbizzani, M. Biso, D. Cericola, M. Lazzari, F. Soavi, M. Mastragostino, J. Power Sources 185 (2008) 1575–1579.
[8] M. Anouti, L. Timperman, M. el Hilali, A. Boisset, H. Galiano, J. Phys. Chem. C 116 (2012) 9412–9418.
[9] R. Lin, P.L. Taberna, S. Fantini, V. Presser, C.R. Perez, F. Malbosc, N.L. Rupesinghe, K.B.K. Teo, Y. Gogotsi, P. Simon, J. Phys. Chem. Lett. 2 (2011) 2396–2401.
[10] W.-Y. Tsai, R. Lin, S. Murali, L. Li Zhang, J.K. McDonough, R.S. Ruoff, P.-L. Taberna, Y. Gogotsi, P. Simon, Nano Energy 2 (2013) 403–411.
[11] D. Pech, M. Brunet, H. Durou, P. Huang, V. Mochalin, Y. Gogotsi, P.L. Taberna, P. Simon, Nat. Nanotechnol. 5 (2010) 651–654.
[12] D. Pech, M. Brunet, T.M. Dinh, K. Armstrong, J. Gaudet, D. Guay, J. Power Sources 230 (2013) 230–235.
[13] S. Hashmi, R. Latham, R. Linford, W. Schlindwein, Ionics 3 (1997) 177–183.
[14] P.L. Taberna, P. Simon, J.F. Fauvarque, J. Electrochem. Soc. 150 (2003) A292–A300.
[15] J. Chmiola, C. Largeot, P.L. Taberna, P. Simon, Y. Gogotsi, Science 328 (2010) 480–483.
[16] C. Shen, X. Wang, W. Zhang, F. Kang, J. Power Sources 196 (2011) 10465–10471.
[17] D. Pech, M. Brunet, P.L. Taberna, P. Simon, N. Fabre, F. Mesnilgrente, V. Conedera, H. Durou, J. Power Sources 195 (2010) 1266–1269.
[18] Y. Jiang, Q. Zhou, L. Lin, Proc. 22nd International Conference on MEMS, 2009.
[19] W. Gao, N. Singh, L. Song, Z. Liu, A.L.M. Reddy, L.J. Ci, R. Vajtai, Q. Zhang, B.Q. Wei, P.M. Ajayan, Nat. Nanotechnol. 6 (2011) 496–500.